088 **PRELIMINARY EXPERIMENTS ON VIRTUAL SOURCE FOR LATERAL MODULATION.**

C Sumi[1*], N Matsui[1], K Shimizu[1], Y Takanashi[1].

Sophia University, 7-1, Kioicho, Chiyodaku, Tokyo, 102-8554 JAPAN.

Submitted for publication in final form: September 17, 2009.

1. Introduction

Originally, an ultrasound (US) virtual source was applied for increasing a lateral resolution and a transmission US intensity in a conventional B-mode imaging [1], in which the first application is also referred to. That is, the virtual source is set at a focus position of a physically large aperture, a synthesized aperture or an individual element aperture. However, the virtual source must remove its neighborhood from a region of interest (ROI). However, in our newly developed virtual source [2], because a virtual source is set backward to the US transducer, such a shallow region to be removed is not generated. Then, superficial tissues such as skin will also be dealt with. In this study, VS1 is applied to a lateral modulation (LM) [2]. Lateral modulations (LMs) have previously been reported using various beamforming methods, and these methods permit B-mode imaging with a high lateral resolution and accurate measurement of a displacement vector using the multidimensional cross spectrum phase gradient method (MCSPGM), multidimensional autocorrelation method (MAM) and multidimensional Doppler method (MDM) (e.g., [3]).

Recently, we also proposed another virtual source that is realized by a random scatters [3] and mirror setting of steered beams [4,5]. Because a summation of random scattering echo is performed, a virtual source may not always be set at the focus positions as in the original virtual source, i.e., an arbitrary position regardless the focus positions. This will increase the applications of a virtual source as discussed later. In addition, the mirror setting is realized using ASTA, i.e., a new beamforming (transmission/reception of ultrasound) method. ASTA is proposed to enable measurements of lateral displacement and of an arbitrary displacement vector with a very high accuracy. This method involves the steering of beams through a steering angle (ASTA) [4,5].

With ASTA, displacement vector measurements can be made, but the number of available methods is limited, and being dependent on the measurement method, only a lateral displacement measurement can be made even if the methods are multidimensional ones. That is, for a displacement vector measurement, our previously developed block matching methods under the assumption of a local rigid motion [6], i.e., multidimensional cross-spectrum phase gradient method (MCSPGM), and multidimensional autocorrelation method and multidimensional Doppler method using a block matching (i.e., MAMb and MDMb, respectively), and for a lateral displacement measurement, in addition to the block matching methods, our previously developed multidimensional autocorrelation method (MAM) and multidimensional Doppler method (MDM) [6] using a mirror setting of the obtained, steered beams [4,5], and one-dimensional (1D) method such as an autocorrelation method can be used. For a lateral displacement measurement, the mirror setting with the multidimensional methods yields the most accurate measuremnt as will be shown.

Thus, in this report, after reviewing the new virtual sources, on an agar phantom experiment, the feasibilities of a lateral modulation B-mode imaging, displacement vector/strain tensor measurements and a shear modulus reconstruction were confirmed, whereas the effectiveness of the mirror setting will be briefly shown through simple simulations.

2. New virtual sources

As shown in Fig. 1a, the setting of a virtual source backward to the transducer array [2] yields a larger transmitted ultrasound intensity by firing plural elements than a physical source used in the classical SA. This virtual source is refereed to as VS1. When using an array aperture, although the original virtual source [1] set in the focus position also gains the transmitted US intensity using plural transmission elements than a physical source (i.e., one element of array) for a classical SA, VS1 gains more effectively the transmission intensity than the original virtual source. Then a larger echo SNR can be obtained. In addition, VS1 does not decrease the axial length of ROI but increases the range of an ROI. In this report, new virtual sources are dealt with as point acoustical sources. Then, a spherical wave is considered as a generated wave. Thus, in this case, the transmitted US from the respective elements is weighted by decay weights that are determined by the reciprocal of the distance from the virtual source and the respective transmission elements. Using the idea of a superposition, VS1 can also be used in a real-time beamforming (not in SA). Other types of virtual sources from the point acoustical source are discussed later.

Otherwise, our previously proposed another virtual source (VS2) is realized by a random scatter in

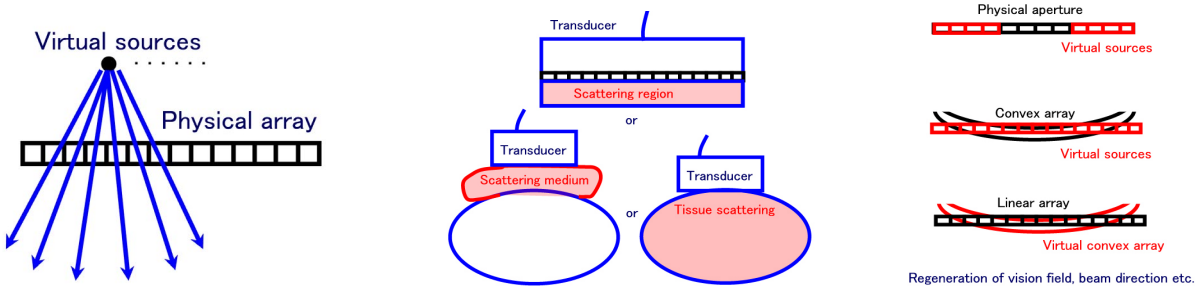

(a) (b) (c)

Fig. 1. New VS's. (a) VS1, and (b) and (c) VS2.

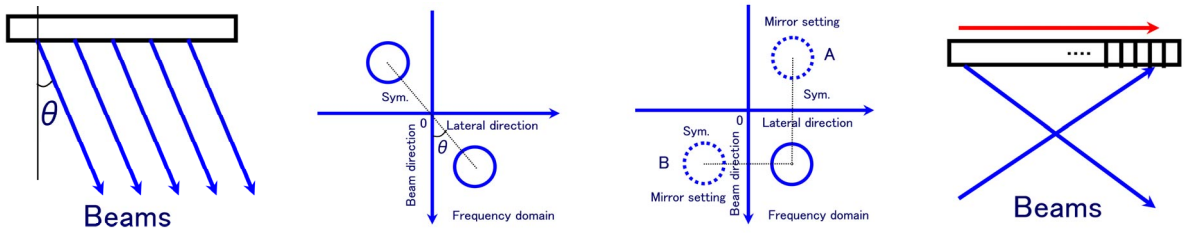

(a) (b) (c) (d)

Fig. 2. Mirror setting. (a) ASTA. (b) A single quadrant spectra. Mirror setting (c) in a frequency domain and (d) a spatial domain.

a random scattering medium (material or target), which can be realized regardless the focus position of a physical aperture but in the neighborhood of the physical aperture. Specifically, VS2 is realized by installing the medium in the transducer, putting it between the transducer and the target body, or in a target medium [3] (Fig. 1b).

In addition to VS1 and VS2, virtual sources (or receivers, VS3) that are realized in null spaces aside the short physical array aperture by searching for the corresponding echo data in acquired echo data set (Fig. 1c) will also increase the application of virtual sources. Then, a lateral width as well as an axial length of a vision of field (VOF) will also increase. Because when a transducer has a small physical array aperture, LM cannot deal with deeply situated tissues [3], new virtual sources will be used for mitigating such a limitation. Alternatively, an arbitrary shape of a VOF will be obtained regardless the physical aperture geometry (see Fig. 1c again, convex, linear etc).

In this study, we also use the mirror setting of steered beams. In ASTA for a 2D region of interest (ROI), as shown in Fig. 2a, steered beams with a steering angle (ASTA) are formed. For proper beamforming, apodization and focusing is performed for transmission and dynamic reception focusing. By slanting a linear 1D array transducer, the ASTA can also be realized mechanically. For a 3D ROI, similarly, such steered beams with a steering angle can be realized by using a 2D array transducer. The results, shown in Fig. 2b, for a single quadrant and single octant (omitted) spectra are obtained for the 2D and 3D ROIs, respectively. That is, for both cases, two symmetric spectra are obtained.

When using the aforementioned block matching methods (i.e., using a least squares estimation) [6] and multidimensional cross-correlation method for both types of beamforming (i.e. ASTA and LM), a 2D or 3D displacement vector measurement can be performed. Also recall that when using LM, a displacement vector can also be measured by using MAM and MDM using no block matching but a moving average [6], and a combination of 1D methods and demodulation methods or our recently reported demodulation method (see Appendix B) [4,5]. For the displacement vector measurements, only an attachment of an US transducer onto a target surface is required.

When using ASTA, for only a lateral displacement measurement, the aforementioned block matching methods can be used at least. However, by performing the quasi-lateral modulations [4,5], because plural independent equations can be obtained, MAM and MDM using no block matching [6] can also be used.

That is, as shown in Fig. 2c, by setting the spectra symmetrically, i.e. specifically at the position A or B, a rf image superposed by an original rf image and the axially (Fig. 2d) or laterally (omitted) inverted rf image is obtained. For a steered beam or local steered beams, by using the mirror setting in a frequency domain or superposing the inverted beam or in a spatial domain, a quasi-lateral modulation can be performed. Because when the target moves in an axial direction, a conventional axial displacement measurement method (i.e., 1D measurement methods such as 1D AM) can be used, and then the quasi-lateral modulation is performed as shown in Fig. 2d for a lateral displacement measurement using MAM or

MDM. For such a quasi-lateral modulation, all block matching methods can also be used.

Such a lateral displacement measurement is a very important application for ASTA (for instance, in measuring blood flow in a vessel running in a direction parallel to the body surface, e.g., carotid artery). For such measurement, *a lateral coordinate must correspond to the direction of the target lateral motion to increase the measurement accuracy*, although usually, the direction of beam should coincide with that of motion by slanting a US transducer, particularly, when using 1D methods (i.e., only division of an instantaneous phase difference by an instantaneous lateral frequency). Thus, ASTA allows providing a simpler manual technique for a medical doctor than such a conventional 1D measurement technique.

Next, the qualities of the beams formed by ASTA and LM are compared. For LM, the following properties may lead to the deterioration of measurement accuracy:

(1) For a measurement in a 2D or 3D ROI, when a classical synthetic aperture (SA) is used, the US intensity transmitted from an element is small, which may yield low SNR echo data. Then, VS1 is required for SA.

(2) Alternatively, when crossed beams are superimposed, although a large US intensity can be obtained, time differences between the transmission of the beams can cause measurement errors, if the displacement occurs during these time differences.

(3) If plural beams which have different paths are used, the inhomogeneity of tissue properties affects beamforming. Specifically, propagation speed affects focusing (i.e., a beam-cross position), whereas attenuation and scattering lead to different frequencies of the respective beams. Then, a phase aberration correction is required, although the experimental results about VS1 and VS2 shown later suggest that the inhomogeneity will not lead to serious problems.

(4) At the minimum, more time is required to complete a beamforming than that required with ASTA. Occasionally, more time is also required to complete a displacement calculation than that required with ASTA.

(5) If obstacles such as a bone exist in a superficial region, a deeply situated tissue cannot be dealt with, because a larger physical aperture is required than that for a conventional beamforming.

In contrast, with ASTA, any of the above concerns, (1) to (4), will not become a problem, (5) will be mitigated, and a simple beamforming increases the ability to make real-time measurements together with a higher accuracy in a displacement measurement.

3 Experiments for VS1 and VS2

Experiments are performed using the same agar phantom as that used in [3]. The target agar phantom [40 (axial, x) x 96 (lateral, y) x 40 (elavational) mm^3] had a central circular cylindrical inclusion (dia., 10mm; depth, 19 mm) with a shear modulus different from that of the surrounding region, and shear moduli of 2.63 and 0.80 x 10^6 N/m^2 in the inclusion and surrounding regions, respectively (i.e., relative shear modulus, 3.29). Manually, the phantom was compressed by 2.0 mm in the lateral direction. The contact surfaces of the linear array type transducer (7.5 MHz, 0.2 mm US element pitch, 2.4 mm depth for acoustic lens involving matching layers) and phantom were separated by less than 0.3 mm by immersing them in water in a tank. A rectangular ROI 13.7 (axial, x) x 13.2 (lateral, y) mm^2 was centered on the inclusion (depths from 12.2 to 25.9 mm).

The depth of a lateral line in which point virtual sources were set was changed from –19.0 mm to 9.0 mm with respect to the linear array surface (0.0 mm). The minus and plus positions respectively correspond to the backward and forward positions from the array surface (i.e., VS1 and VS2). For LM, the same parabolic modulation was performed as that described in [3]. An achieved lateral modulation frequency was 3.75 MHz.

Fig. 3a shows the B-mode image and the images of lateral and axial displacements (i.e., dy, dx), a relative 2D shear modulus reconstruction, and lateral, axial and shear strains obtained for (upper) physical sources (i.e., 0.0 mm depth), (middle) -3.0 mm (VS1), and (lower) 3.0 mm (VS2) that a specular can be seen at the same circled position. For the range, a relative shear modulus could be estimated with a high accuracy (≈ 3.3). The means and SDs of (a) reconstructed relative shear moduli and (b) measured strains in the inclusion are shown in Fig. 3b. Although not shown, for 0 mm depth physical source, when LM and a superposition of steered beams [3] are performs, almost the same reconstruction and measurements were obtained (e.g., the same means and SDs with 10^{-3} order). See Table VIII in [3].

4 Simulations for mirror setting

Simple simulations regarding a lateral displacement measurement were performed. Echo data were simulated by generating a Gaussian type PSF with white data in a 2D ROI. For the lateral motion (0.01 mm), a steering angle (Fig. 2a) for ASTA was set at 45 degrees. For LM, a steering angle of –45 degrees was also used. The US frequency was changed from 3.5 to 12 MHz under these conditions including an US speed of 1,500 m/s; an axial sampling interval of 0.05 mm; and a beam pitch of 0.05 mm. By adding white noise data to the raw echo data, echo data with a SNR of 20dB was also simulated.

For ASTA and LM, the means and/or SDs obtained are shown in Fig. 4, specifically, (a) obtained by

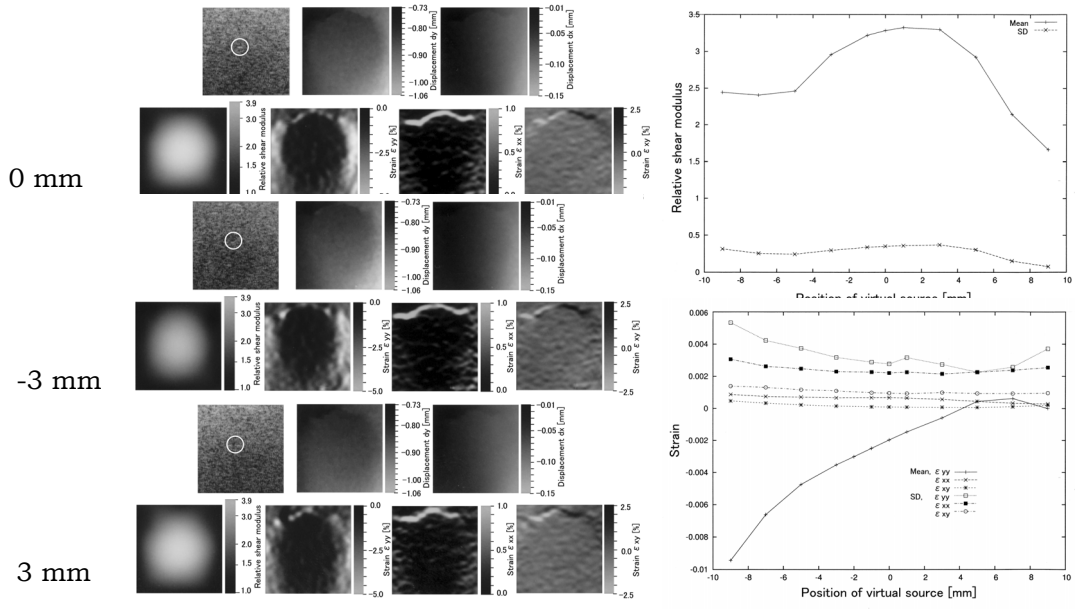

(a) (b)

Fig. 3. Agar phantom experiments (a) 0, -3, and 3mm. (b) Virtual source position vs means and SDs of reconstructed shear moduli and measured lateral strains in inclusion.

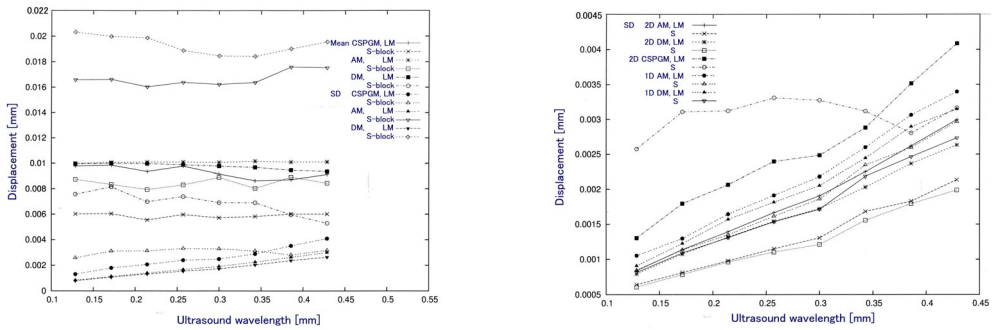

(a) (b)

Fig. 4. For ASTA and LM, means and SDs of lateral displacement measurement vs lateral frequency obtained using (a) displacement vector measurement methods and (b) lateral displacement measurement methods.

displacement vector measurement methods (i.e., MCSPGM, MAM, MAMb, MDM and MDMb) and (b) obtained by lateral displacement measurement methods (i.e.,mirror setting with MAM and MDM, MCSPGM, and demodulation with 1D methods, and 1D methods). For all measurements, high measurement accuracies are achieved using a high lateral frequency (see Appendix C for increasing the lateral frequency). The order of measurement accuracy is in (a), (LM+MAM, MDM)>(LM+MAMb, MDMb, MCSPGM)>(ASTA+MAMb, MDMb, MCSPGM), and in (b), (ASTA+Mirror setting+MAM, MDM)>(LM+MAM, MDM)>(ASTA+1D methods)>(LM+1D methods). Thus, for a displacement vector measurement and a lateral displacement measurement, ASTA and LM, LM and ASTA are proper beamformig, respectively. For a displacement vector measurement, a block matching yields a lower accuracy measurement than a moving average. For both measurements, 1D methods yield lower accuracy measurements than the corresponding multidimensional methods.

5. Discussions and conclusions

In this report, for our newly developed virtual sources VS1 and VS2, preliminary experimental results were presented for a lateral modulation (LM). However, no long range of a virtual source depth could not be obtained for the used ultrasound transducer.

However, in this study, the noises filled in the acquired echo data for SA were also weighted together with original echo signals by the decay weights. That is, the improvement in an echo SNR achievable by SA is not strictly shown yet. In the near future, the smaller pitch of US elements will be used. Such an improvement will increase the range of a virtual source depth. Because our newly developed virtual sources will also mitigate the problem of a rapid motion, dynamic experiments will also be conducted.

Aforementioned other applications will also be achieved with a consideration of the results obtained.

In addition, for VS1 and VS2, we'll also conduct the use of another virtual source that is not a point source, for instance, one having a finite aperture. That is, decay weights will be calculated analytically or numerically. Moreover, our developed optimization method for determining the beamforming parameters such as an apodization function involving delays will also be used to determine the position of virtual sources.

Next, for the mirror setting, we performed simulations. Considerations of the beamforming schemes using LM and ASTA show that the simple ASTA beamforming method increases capabilities for real-time measurements when compared with LM, and a two-dimensional echo simulation shows that except for the block matching methods, ASTA yields more accurate displacement measurements than LM. For a lateral displacement, the mirror setting yields the most accurate measurement. Moreover, as with LM, multidimensional measurement methods yield more accurate measurements than the corresponding 1D measurement methods. For measurements, although a block matching requires fewer calculations than a moving-average, however, lower accuracy measurements are obtained. Being dependent on the echo SNR and the local region (window) size, as for LM [3], a proper measurement method should also be selected for ASTA. Thus, ASTA will open new aspects of displacement measurements together with LM.

Appendix A. New demodulation method for displacement vector measurement using LM and 1D measurement methods

When LM is performed, demodulation methods reported by Anderson and Jensen can be used together with a 1D measurement method. We also developed a new demodulation method ("CONJ PRODUCT" used in section 4 [4,5]). For example, when a 2D displacement vector (dx,dy) is measured, after obtaining instantaneous phase differences between pre- and post-motions in exponential form [e.g., expj(fxdx+fydy) and expj(fxdx-fydy)], by calculating their product and their conjugate product, exp j(2fxdx) and expj(2fydy) are obtained. Thus, by dividing their phase differences by the respective frequencies 2fx and 2fy in 1D measurement methods, the displacement vector (dx,dy) can be obtained. Note that because twofold instantaneous frequencies are used, large bandwidths should be used in advance (Nyquist theorem) or an increase in bandwidth (interpolation) must be performed as described in Appendix B. This method can be extended simply to a 3D displacement vector measurement, in which the twofold instantaneous frequencies appears similarly after handling of three or four instantaneous phase differences between pre- and post-motions in exponential form.

Appendix B. Increase in lateral frequency by an increase in steering angle

For LM and ASTA, to achieve a high lateral frequency, it is necessary to increase the beam steering angle. However, when the pitch of the element or beam is not small enough, an aliasing of spectra occurs in a frequency domain. To mitigate the occurrence of aliasing, the beam pitch is kept appropriately small. For LM using the superposition of plural steered beams and ASTA, the respective beams are interpolated in a frequency domain by increasing a lateral bandwidth (BW) padded by zeros [4,5]. In conjunction, the separation of overlapped beams in a spatial domain such as crossed beams (LM), grating lobes, side lobes and signals received from some source can be separated in a frequency domain. These separations in a frequency domain are effective for echo imaging and displacement measurements. For LM and ASTA, when a beamforming (transmission/reception of US) is preformed, after receiving echo signals in SA, or after obtaining steered beams, by rotating the coordinate in the spatial or frequency domain, the axial, lateral and elevation frequencies can also be controlled. Figure 5 shows (a) a B-mode image and spectra when aliasing occurs in ASTA (0.3 mm pitch beams), of which a lateral bandwidth is increased [(b), fourfold], with which a lateral modulation is performed [(c)].

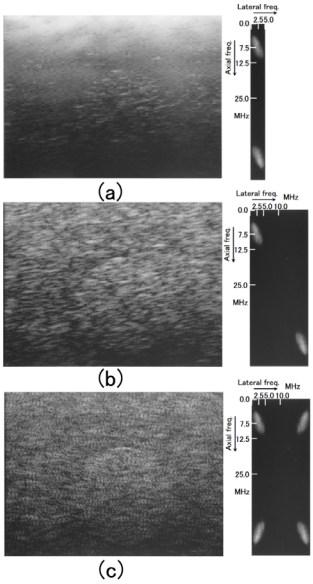

Fig. 5. Increase in BW.

References

1. C. H. Frazier et al., IEEE Trans UFFC 45 (1998) 196.
2. C. Sumi et al., Proc.2009 Spring Meet Acoust Soc Jpn (March 2009) 1381.
3. C. Sumi, IEEE Trans UFFC 55 (2008) 2607.
4. C. Sumi et al., "Applications of ultrasonic beam steering to tissue imaging," IEICE Technical Report US2009-28 (July 2009) 33-37.
5. Submitted.
6. C. Sumi, IEEE Trans UFFC 55 (2008) 24.